Journal of New Materials for Electrochemical Systems 13, 305-313 (2010)

Flow Rate Effect on Methanol Electro-oxidation in a Microfluidic Laminar Flow System

Isaac Sprague[1], Prashanta Dutta[1] and Su Ha[2,*]

[1]School of Mechanical and Materials Engineering, Washington State University, Pullman, WA 99164-2920, USA
[2]School of Chemical Engineering and Bioengineering, Washington State University, Pullman, WA 99164-2710, USA

Received: July 30, 2009, Accepted: March 30, 2010

Abstract: *The effect of flow rate on the methanol electro-oxidation reaction in laminar flow was investigated using a direct methanol laminar flow fuel cell (LF-FC). A micro fuel cell was fabricated in polydimethylsiloxane using standard soft-lithography techniques. The electrochemical performance of methanol oxidation was characterized by anode polarization and electrochemical impedance spectroscopy analysis with and without sulfuric acid. The results show that in the absence of a sulfuric acid electrolyte (H_2SO_4) the methanol flow rate significantly influences methanol oxidation kinetics of the laminar flow direct methanol fuel cell. In the absence of H_2SO_4, it was found that the charge transfer resistance and onset potential of the methanol oxidation reaction significantly increases as the methanol flow rate increases. As a result, the anode current density of LF-FCs decreases at higher flow rates of methanol. However, this negative effect was reduced when a strong electrolyte, such as sulfuric acid, was mixed with the methanol solution.*

Keywords: anode polarization, electrochemical impedance spectroscopy, microfluidic fuel cell

1. INTRODUCTION

Demand for new sources of portable power has given rise to a renewed interest in fuel cell technology. There have been efforts to miniaturize existing polymer electrolyte membrane (PEM) fuel cells to replace conventional batteries. Given the small sizes that would be required, this is not an easy or straightforward task. However, a new fuel cell system has been developed with the small size necessary to meet market demands; a microfluidic fuel cell. These devices, referred to as laminar flow fuel cells (LF-FCs), consist of a fuel stream and an oxidant stream flowing in a single microchannel [1]. Because of the nature of flow in a microchannel, the streams can only mix via diffusion and thus the anode and cathode reaction are kept separate while still allowing the necessary ion exchange.

Many articles have been published focusing on device design for maximizing the power density of LF-FCs. Initial LF-FCs used a Y-channel type design [2-3] and planar channels [4]. To capitalize on the fuel flexibility of LF-FCs and improve their thermodynamic potentials, different combinations of anode and cathode solutions have been studied [5-9]. In order to improve the oxygen mass transport at the cathode, modifications of LF-FCs with an air breathing cathode have also been investigated [10-11]. Additionally, devices with multiple laminar streams [12] and different electrode configurations have been studied [13-14].

Similar to conventional fuel cells, the performance of LF-FCs is limited by kinetic, ohmic and mass transport overpotentials. The performance limitations of LF-FCs have been investigated [15] and special attention paid to the electrode diffusion layer limitation [16]. Since fuel cells are complex systems, figuring out how each of these limitations affects the overall performance is not trivial. There are several experimental techniques, such as electrode polarization and electrochemical impedance spectroscopy, which provide in-situ characterization of these limitations. Impedance spectroscopy is a relatively new and powerful method for characterizing many of the electrical properties of materials and their interfaces. Recently, this analytical method has been used to evaluate the electrochemical behavior of anode and cathode electrodes, as well as electrolyte materials of hydrogen fuel cells and direct liquid fuel cells [17-22].

In a typical PEM fuel cell the electrolyte is stationary, whereas in a LF-FC the electrolyte is a flowing stream. This could potentially give rise to new unstudied performance limitations of LF-FCs, as a moving electrolyte is unique. Also, unlike conventional

*To whom correspondence should be addressed: Email: suha@wsu.edu

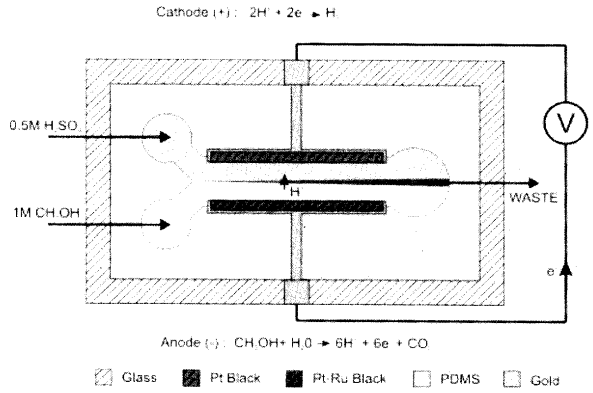

Figure 1. Schematic of the laminar flow fuel cell used to study its anode performance.

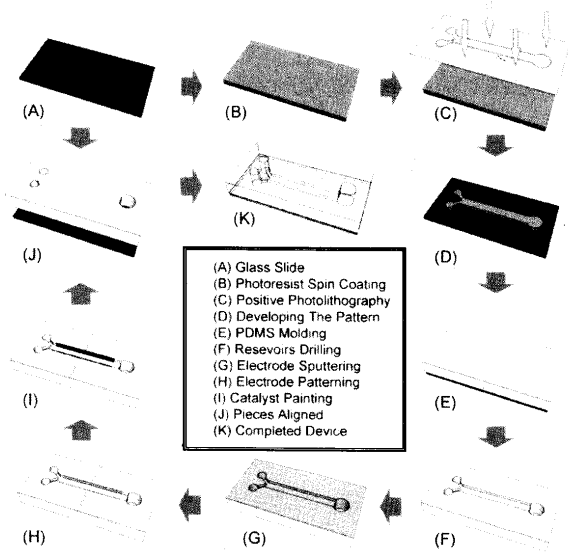

Figure 2. Fabrication sequence of the laminar flow fuel cell (LF-FC).

PEM fuel cell systems where the fuel feed is physically separated from the electrolyte, the electrolyte and fuel streams in LF-FC are the same. This means that the electrolyte strength of the fuel stream plays an important role in the device performance for LF-FCs. Therefore, the fuel selection must be carefully considered as not all fuels are good electrolytes. For example, while both the formic acid and methanol are simple hydrocarbon fuels, methanol is not a good electrolyte. Often a strong electrolyte, such as sulfuric acid (H_2SO_4), can be added to the methanol solution to improve its poor electrolyte property. However, this modification may not be acceptable in all cases, such as enzymatic biofuel cells where the strong electrolyte deactivates the enzymes. It is scientifically important to understand how the electrolyte strength of the fuel stream affects the electrochemical performance, especially in the context of this unique case where it is also flowing. In this study, the focus was placed on the electrochemical oxidation reaction of LF-FCs and how it is affected by different flow rates of the anode stream. Methanol was selected as the model fuel because it allows us to study the performance of LF-FCs in a case where the fuel has poor electrolyte properties. Sulfuric acid was also added to increase its electrolyte strength and understand how the presence of strong supporting electrolyte in the anode stream can alter its electrochemical performance.

2. EXPERIMENTAL SECTION

2.1. Design of Device

A device schematic with a simple depiction of laminar flow is shown in Figure 1. The device was used to study the anode electrochemical performance of LF-FCs. To isolate the anode, the straight channel was made 3 mm wide and 10 μm tall which yields a relatively large separation between electrodes. This wide channel insures complete separation between the anode and cathode such that no mixed potentials occur over these two electrodes and that there is minimal mixing between the two streams. The distance a species will diffuse from one stream into the other, known as the transverse diffusive broadening, is given by [23, 24]:

$$\delta(y) \propto \left(\frac{DHx}{U}\right)^{1/3} \quad (1)$$

where x is the distance along the channel from where the streams meet, D is the diffusivity of the species, H is the channel height, and U is the average fluid velocity in the channel. Assuming a diffusivity coefficient of 1×10^{-9} m^2/s and an average velocity of 1.11 mm/s (corresponding with a reactant flow rate of 1 μL/min), the transverse diffusive broadening at the exit of the channel (x = 25 mm) is 60.8 μm which is significantly less then the total channel width of 3 mm. Consequently, the cathode solution will not significantly mix with the anode solution. The anode operating conditions are only affected by the anode stream and are completely independent of the cathode conditions.

Referring to Figure 1, the straight channel is 25 mm long, while the branch channels of the Y-junction are 1.5 mm wide and 5 mm long. Each reservoir is 5 mm in diameter. The LF-FC was made with polydimethylsiloxane (PDMS) on a glass substrate. The gold electrodes are deposited on both sides of the channel with dimensions of 20 mm long, 0.5 mm wide, and 375 nm thick. The anode and cathode catalysts are Pt-Ru Black and Pt Black respectively. Pt-Ru was used at the anode to limit CO poisoning, which is a poisoning intermediate for methanol oxidation.

2.2. Fabrication of Laminar Flow Fuel Cell

Figure 2 shows the steps involved in fabricating the device. A positive mold was made on a glass slide, shown in Figure 2.A, using standard photolithographic techniques. Briefly, photoresist was spun on (Figure 2.B), and patterned using positive lithography (Figure 2.C&D). PDMS prepolymer and curing agent (Sylgard 184, Dow Corning Inc., Midland, MI) were mixed with a ratio of 10:1 and poured onto the mold. The PDMS then degasses for 2 hours at 0.001 Torr and baked at 80°C for 3 hours (Figure 2.E). The PDMS channel was removed from the mold and trimmed to size. The reservoirs were formed using a 20 gauge needle to punch out a hole in the PDMS (Figure 2.F). The gold for the electrode was sputtered to 375 nm thick layer using a 10 nm TiW layer as an adhesion layer (Figure 2.G). The electrodes were then formed by standard gold

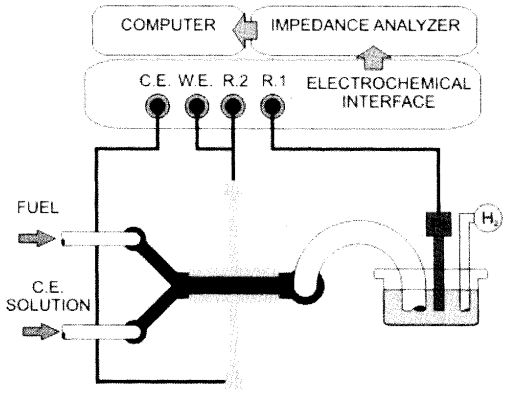

Figure 3. Experimental setup for electrochemical impedance spectroscopy of the anode in a LF-FC.

patterning techniques (Figure 2.H). Catalyst inks were prepared by mixing appropriate amounts of catalyst particles, Millipore water, and Nafion® solution. This mixture was sonicated and applied to the gold electrodes using a brush and heat lamp to evaporate the excess water (Figure 2.I). The PDMS channel was exposed to oxygen plasma and placed on a glass slide (Figure 2.J), using slight pressure and allowed to sit for 24 hours creating a permanent bond and the final device, Figure 2.K. Capillary tubes were then glued in the reservoirs for transport of reactants and products to and from the device, respectively. Wires were cold soldered using silver conductive epoxy (MG Chemicals, Burlington Ontario) to form the electrical leads of the fuel cell.

2.3. Materials and Reagents

HPLC grade methanol and sulfuric acid were purchased from Aldrich (St. Louis, MO). Platinum black and platinum-ruthenium black (50:50 atomic %) were purchased from Alfa Aesar (Ward Hill, MA). Nafion (5% Solution) was obtained from Solution Technology Inc (Mendenhall, PA). The fuel and oxidant solutions were prepared in the laboratory. For the fuel, methanol was diluted with Millipore water to a concentration of 1 M. For the oxidant, sulfuric acid was diluted with Millipore water to a concentration of 0.5 M.

2.4. Test of Fuel Cell

To study the effect of the anode flow rate with different electrolyte strengths on the anode performance of LF-FCs, 1 M methanol solution, with various concentrations of sulfuric acid, were supplied to the anode inlet reservoirs. Methanol, in the absence of sulfuric acid, represented a fuel stream with poor electrolyte strength while a solution of methanol and sulfuric acid represented a stream with good electrolyte strength. A 0.5 M sulfuric acid solution was fed to the cathode. Reaction by-products CO_2, water, and unutilized fuel were collected as waste in the exit reservoir. These solutions were pumped through the device using a syringe pump (74900-10, Cole-Parmer Instrument Company, Vernon Hills, IL) at flow rates of 1, 2, or 3 μL/min. In all tests performed, the flow rates of the anode and cathode streams were identical and equal to the flow rate specified by the operating conditions. Also, the cell was allowed to run for an hour for the flow to reach a steady state.

2.5. Anode Polarization

To characterize the anode performance, an anode polarization was performed. First, the fuel and oxidant solutions were supplied and the cell was allowed to reach steady state. Then an incremental voltage was applied across the cell using a system power supply (6033A, Hewlett Packard, Palo Alto, CA). Figure 1 shows the set up for this test. The applied voltage was increased from 0 to 800 mV in 50 mV steps at 30 second intervals. The current in the circuit was measured with a multimeter (187, Fluke Corporation, Everett, WA). In this configuration, the methanol is electrochemically oxidized at the anode. The cathode, however, acts as a dynamic hydrogen reference electrode (DHE), providing both a counter and reference electrode for the study. This means that the anode polarization test allows the measure of performance limitations associated with the anode electrode only.

2.6. Electrochemical Impedance Spectroscopy

For the electrochemical impedance spectroscopy, the cell was again supplied with fuel and oxidant and allowed to reach a steady state flow. A 0.5M of sulfuric acid solution was supplied to the cathode. This allows us to eliminate the effect of the cathode impedances and to investigate only the anode impedances of the cell as the cell operation parameters are varied.

To perform the measurements, the cell was connected to an electrochemical interface (SI 1287, Solartron Analytical, Farnborough Hampshire, UK). The electrochemical interface was connected to an impedance/gain-phase analyzer, (SI 1260, Solartron Analytical, Farnborough Hampshire, UK) as shown in Figure 3. The impedance analyzer was linked to a computer and controlled using ZPlot (Scribner Associates Inc, Southern Pines, NC).

The cell was connected to the electrochemical interface as a three terminal cell. Due to the sensitivity of this technique, it was beneficial to separate the reference electrode from the counter electrode in these experiments. To accurately control the potential of the working electrode, the reference electrode was needed in the electrolyte. This was accomplished with a standard hydrogen reference electrode placed in the waste beaker. The beaker was filled with 1 M sulfuric acid and hydrogen was bubbled onto a platinum wire. This setup is appropriate as there is a direct electrolyte connection between the reference electrode and working electrode. Also, because no current flows between the working electrode and the reference electrode, any potential drop between the two electrodes is negligible. Next, the working electrode and second reference electrode leads of the interface were both connected to the anodic side of the device. Finally, the counter electrode lead was connected to the cathodic side of the cell. The lines were kept short and laid in an orderly fashion to avoid stray inductance amongst wires.

For the impedance measurements, a frequency sweep was performed with potential as the input, and current as the measured quantity. The amplitude of the AC potential signal was 50 mV and the frequency was swept between 1 MHz and 1 Hz. The device was too unstable to get data below 1 Hz with sufficient repeatability. For each set of operating conditions the impedance measurements were performed at a variety of loads. It was found that regardless of the applied load, the observed changes in impedance with respect to both the various anode flow rates and electrolyte strengths were very similar. Thus, only the impedance measurement data at open circuit potential is reported in this paper. All scans were performed

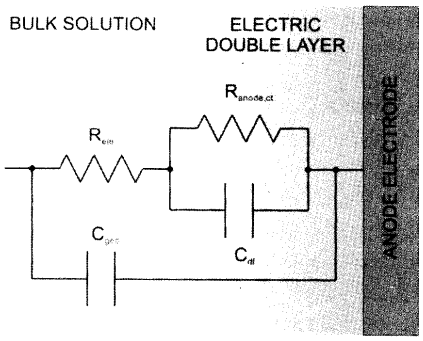

Figure 4. The equivalent circuit that represents the anode electrode of methanol based LF-FC.

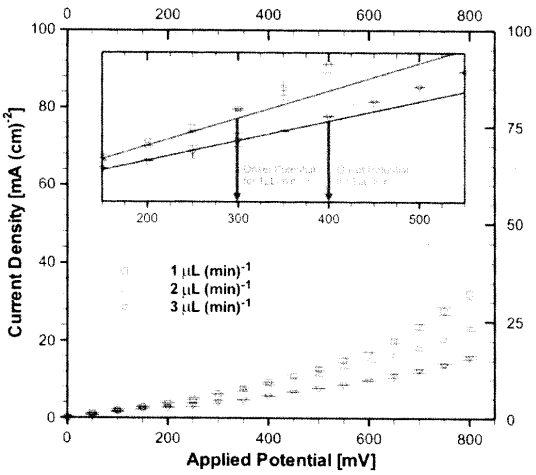

Figure 5. Anode polarization curves of LF-FC at the room temperature with different methanol flow rate. The 1 M methanol solution with no sulfuric acid was used for the anode. The platinum black (PtBl) based cathode was used as a dynamic hydrogen reference electrode/counter electrode.

four times and the average data is presented.

2.7. Equivalent Circuit Model

Electrochemical impedance spectroscopy is a powerful tool that can provide a great deal of revealing information; however the data is difficult to analyze directly. By using an equivalent circuit to recreate the measured impedance spectra, the information learned from the experiments can truly be maximized. The equivalent circuit used to describe the anode electrode in this study is shown in Figure 4. The equivalent circuit for fuel cell electrode kinetics at the electric double layer is a resistor in parallel with a capacitor, where the resistor represents the resistance to charge transfer across the solution electrode interface ($R_{anode,ct}$), and the capacitor represents the capacitance between the electric double layer and electrode surface (C_{dl}). This kinetic circuit is then connected in series with R_{ele}, which represents the resistance to ion conduction in the electrolyte [25]. The final component is the geometric capacitance, or C_{geo}. Often this final component is omitted from fuel cell circuits, but in this case, it must be included because the frequency ranges up to 1 MHz [25]. This capacitance represents the fact that a LF-FC's geometry forms a capacitor because two electrodes separated by a gap is essentially a capacitor. C_{geo} should therefore be constant throughout this study. Another element of the equivalent circuit is the Warburg impedance. This impedance is caused by the diffusion of ions within the cell and predominately shows up at lower frequencies. The impedance is small in the high frequency range because the diffusing reactants don't have to move very far in response to the perturbation signal [26]. This impedance was omitted from the equivalent circuit model in this study because the unstable device behavior at low frequency didn't allow for acceptable data fitting. Therefore, the circuit fitting was done only in a frequency range between 1 MHz and 100 Hz where impedance is not significantly affected by diffusion. The fitting was performed by ZView (Scribner Associates Inc, Southern Pines, NC) with an accuracy of less then 2% error on each calculated value.

3. RESULTS AND DISCUSSION

3.1. Methanol Flow Rate Effect in Absence of H_2SO_4 on Methanol Oxidation Kinetics

First the anode performance was studied with a flowing methanol stream in the absence of sulfuric acid, leading to a flowing poor electrolyte. It was found that at different flow rates the anode performance changed. Figure 5 shows the anode polarization plots of a LF-FC using 1 M methanol in the absence of sulfuric acid at the various flow rates. It shows that as the methanol flow rate increases the anode performance decreases. This is not an expected result because higher flow rates would usually mean better fuel replenishment by decreasing the thickness of mass transport boundary layer and therefore better performance [3]. These results would indicate that a higher methanol flow rate adversely affects methanol oxidation kinetics. In Figure 5, the methanol flow rate of 3 mL/min shows the onset potential of methanol oxidation at around 400 mV vs. DHE. (The onset potential is defined as the applied anode potential that leads to the exponential increase in the anode current density. It can be determined by evaluating at what value of applied potential does the anode polarization deviate from a linear increase.) However, as the flow rate decreases from 3 to 1 mL/min, the onset potential of methanol oxidation decreases from 400 to 300 mV vs. DHE. This trend in Figure 5 suggests that the increased flow rate of methanol negatively affects the methanol oxidation kinetics.

Although it is not convincing to make this conclusion from the anode polarization data alone, the electrochemical impedance spectroscopy data provides further insight into the performance drop at higher methanol flow rates. Figure 6A shows the anode impedance spectrum for different methanol flow rates in the absence of sulfuric acid. At first glance, it shows that as the methanol flow rate increases from 1 to 3 mL/min the overall anode impedance also increases. Also, because the change in impedance is primarily in the second and larger semi-circle, it appears that this increase in impedance is associated with methanol oxidation kinetics.

For a more rigorous analysis of the impedance spectra, the data was fit to the equivalent circuit model. Figure 6B shows the fitted results for the R_{ele} and $R_{anode,ct}$. Figure 6B clearly shows that Ranode,ct increases from 37.4 ohms to 48.1 ohms while C_{dl} decreases from 1.60 to 1.36 mF as the flow rate increases from 1 to 3

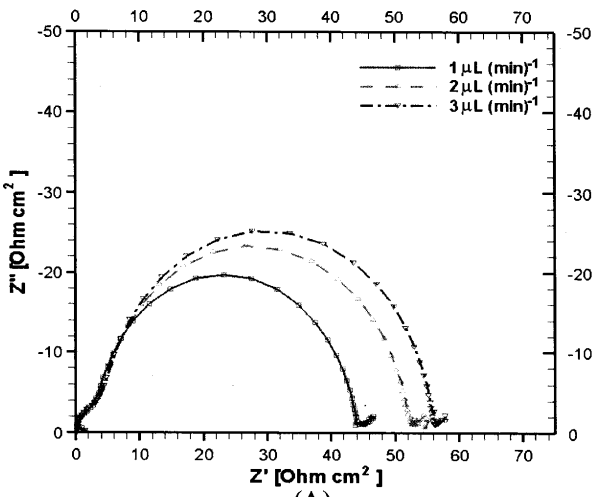

(A)

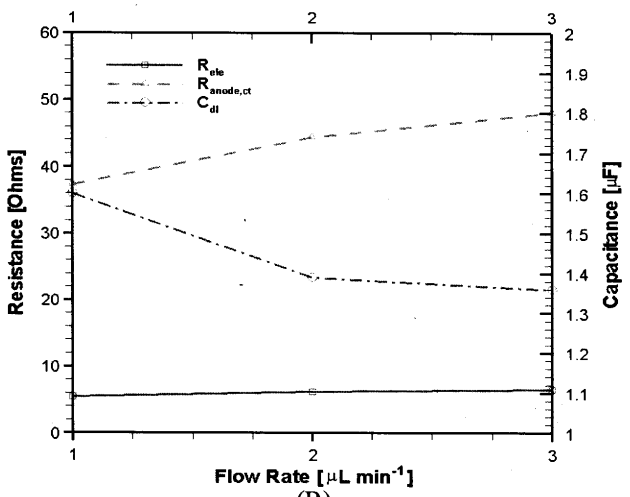

(B)

Figure 6. (A) Anode impedance spectra showing the methanol flow rate effect on the anode performance of LF-FC. Methanol concentration was fixed at 1 M and no sulfuric acid was added. The PtBl cathode was supplied with 0.5 M sulfuric acid and served as the counter electrode. (B) The equivalent circuit fit values of solution resistance (R_{ele}), anode charge transfer resistance ($R_{anode,ct}$) and anode double layer capacitance (C_{dl}) based on Figure 6 (A).

mL/min. It also shows that R_{ele} is essentially unchanged with methanol flow rate. Both Figures 5 and 6 demonstrate that, as the flow rate increases, the onset potential and Ranode,ct of methanol oxidation increases. Thus, it is harder to oxidize the methanol at the anode electrode with the higher methanol flow rate, which leads to the lower anode current output.

The change in Ranode,ct with a lack of change in R_{ele} would indicate that the flow rate effect occurs at the electrode solution interface. From the electroneutrality condition it is easy to deduce that a fluid with zero charge density can have no effect on the ionic current in the solution [27]. Therefore, in the bulk fluid, where the electroneutrality condition applies, there should be no effect of

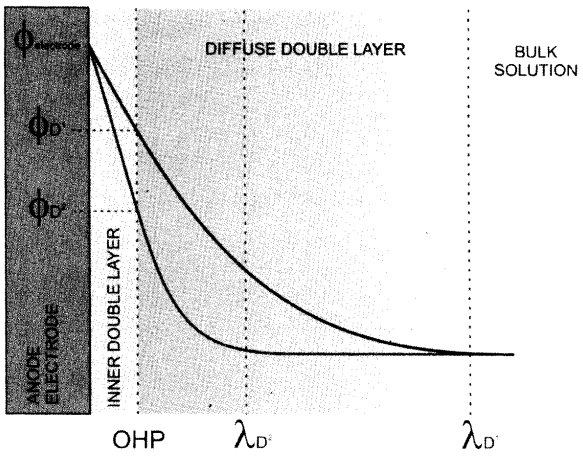

Figure 7. Schematic of two potential distributions across the electric double layer at the electrode-solution interface for a constant electrode potential, $\phi_{electrode}$. The electric double layer consists of two parts, the inner double layer which is from the electrode to the outer Hemholtz plane (OHP), and the diffuse double layer whose width is characterized by the Debye Length. The wider diffuse double layer, having a Debye length of λ_D^1 , has a higher potential at the start of the diffuse double layer, ϕ_D^1 , than the potential for the narrower diffuse layer, ϕ_D^2 , whose Debye length is given by λ_D^2 . This leads to a lower potential drop across the inner double layer for the system with the wider diffuse double layer. Because the potential drop across the inner double layer is the actual driving force for kinetics, the electric double layer with the wider diffuse layer leads to worse kinetics than the electric double layer with a narrower diffuse layer.

flow rate on the conduction of protons across the cell. This is shown by the constant Rele in Figure 6B.

However, at the solution-electrode interface the solution is not electrically neutral, instead it is an imbalance of positive and negative ions leading to a charge density that balances out the charge in the electrode. This region is also referred to as the electric double layer and its width directly impacts electrode kinetics [28]. The electric double layer consists of two parts; the inner double layer (from the electrode to the Outer Hemholtz Plane) and the diffuse double layer. The true overpotential, which is the actual driving force for the electrode kinetics, is the potential drop across the inner double layer [28]. Because the potential gradient must be continuous, a wider electric double layer will yield a smaller potential drop across the inner double layer for the same electrode potential, as shown in Figure 7. Consequently, the anode electrode with a wider electric double layer has a lower kinetic driving force and a greater resistance to methanol oxidation.

The width of the electric double layer is also directly linked to the double layer capacitance. The inner and diffuse double layers are connected in series. As a result, the total capacitance of electric double layer (C_{dl}) is the combination of the capacitance of the inner double layer (C_{inner}) and the capacitance of the diffuse double layer ($C_{diffuse}$) as follows [26]:

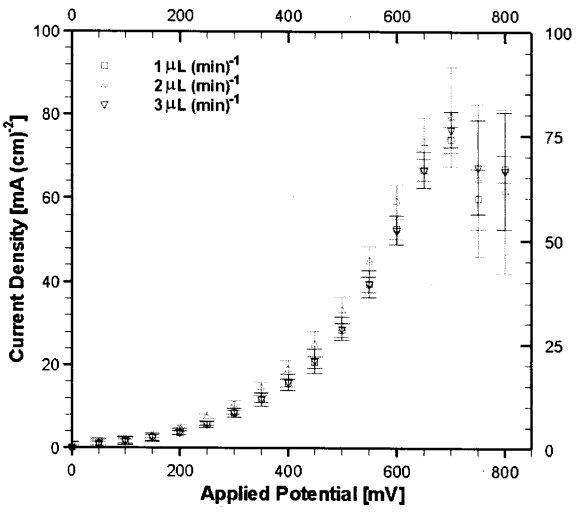

Figure 8. Anode polarization curves of the laminar flow fuel cell at the room temperature with different anode flow rates. The 1 M methanol solution with 0.5 M sulfuric acid was used for the anode. The PtBl based cathode was used as a dynamic hydrogen reference electrode/counter electrode.

$$\frac{1}{C_{dl}} = \frac{1}{C_{inner}} + \frac{1}{C_{diffuse}} \tag{2}$$

The inner double layer is very compact and its capacitance can be assumed to be a constant. However, the diffuse double layer is much wider and its capacitance is given by the Gouy- Chapman model

$$C_{diffuse} = \frac{\varepsilon}{\lambda}\cosh\left(\frac{zF\phi_0}{2RT}\right) \tag{3}$$

where ε is the permittivity of the solution, R is the gas constant, F is the Faraday's constant, z is the charge number of ions, ϕ_o is the electric potential at a standard state, and λ is the Debye length or width of the diffuse double layer [26]. For this system, evidence that the Debye length is changing is shown in Figure 6B where the C_{dl} decreases as flow rate increases. Under the experimental conditions, the values of ε, R, F, z and ϕ_o are constant regardless of the anode flow rates. Therefore, based on Equations (2) and (3), it can be concluded that the increase in flow rate caused the width of the diffuse double layer (λ) to increase which leads to the decrease in the total capacitance of the electric double layer (C_{dl}) as shown in Figure 6 (B). As the width of the diffuse double layer (λ) increases with the higher flow rate, the true activation overpotential across the inner double layer decreases which resulted in slow electrode kinetics. These slow kinetics would lead to the increase in $R_{anode,ct}$ at higher methanol flow rates.

Presently, the exact fundamental explanation of how the width of the diffuse double layer would increase with increasing flow rate is not known. As was mentioned previously, the electric double layer is not electrically neutral, and instead, it has an imbalance of positive and negative ions. The position of these ions is a balance between the diffusion and migration driving forces on the ions [27,28]. Since these ions are in a moving solution, this balance should be affected by the bulk flow and therefore so would the structure of the double layer. Further investigation is required for a more complete answer.

3.2. Methanol Flow Rate Effect in Presence of H_2SO_4 on Methanol Oxidation Kinetics

Assuming that the high electrolyte flow rate does increase the width of the diffuse double layer then adding a strong supporting electrolyte to the methanol solution could mitigate this effect. The Debye length is given by

$$\lambda = \left(\frac{\varepsilon RT}{2F^2z^2C}\right)^{1/2} \tag{4}$$

where C is the bulk concentration of electrolyte in the solution. Therefore, by greatly increasing the concentration of the electrolyte the width of the diffuse double layer is greatly reduced, potentially making it less susceptible to flow rate effects. Figure 8 shows the anode polarization of methanol oxidation in the presence of sulfuric acid at different flow rates. According to Figure 8, both the onset potential and anode current output of methanol oxidation reaction are not significantly influenced by the methanol flow rate. Regardless of the methanol flow rate, with the presence of 0.5M sulfuric acid in the fuel solution, the anode polarization plots are about the same. This would indicate that there is no change in anode overpotentials based on the flow rate of methanol with strong supporting electrolyte.

The impedance data also shows that there is no trend associated with the flow rate of methanol with strong supporting electrolyte. Figure 9A shows the anode electrochemical impedance spectra using the various flow rates of methanol in the presence of 0.5 M sulfuric acid. Figure 9B shows the equivalent circuit fitting results for the same operating conditions. It would appear that the data shows no trend with methanol flow rate. However, it is difficult to be sure of any conclusions from this data because the overall anode impedance is so small that the impedance associated with the cathode starts to become an issue. The equivalent circuit analysis was less effective and yielded relatively high errors, on the order of 100% for $R_{anode,ct}$ and R_{ele} making comparison between flow rates impossible. It is also possible that since the cathode impedance can no longer be neglected, the equivalent model presented in Figure 4 is not sophisticated enough to fully describe the data with 0.5M sulfuric acid in the anode stream. For this study, only the trends in basic anode behavior are important and the equivalent circuit presented in Figure 4 is sufficient if the overall anode impedance is large enough such that the impedance associated with the cathode can be neglected. The cathode impedance can be neglected when good impedance data fitting with the equivalent circuit is obtained. To alleviate this problem of a poor fit at high sulfuric acid concentrations, the electrochemical impedance spectroscopy was performed again with only 0.1 M and 0.05 M sulfuric acid added to the methanol solution. The results from these experiments allowed us to use the equivalent circuit analysis with more confidence. The curves were fit to the equivalent circuit model, which yielded the

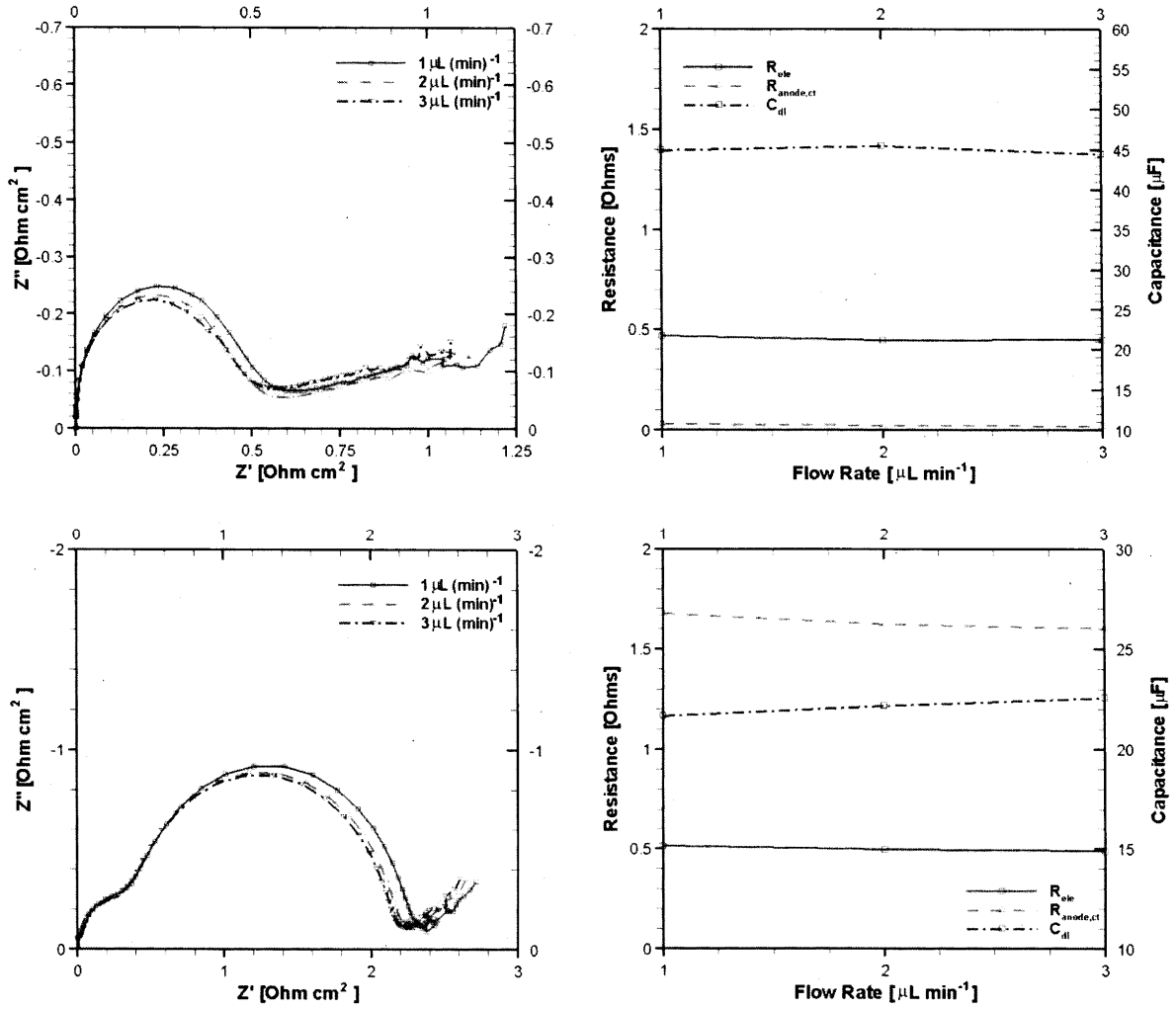

Figures 9. Anode impedance data showing the methanol flow rate effect in the presence of sulfuric acid on the anode performance of LF-FC. Methanol concentration was fixed at 1 M. The PtBl cathode was supplied with 0.5 M sulfuric acid and served as the counter electrode. (A) Impedance spectra for 0.5 M sulfuric acid added to the methanol solution. (B) The equivalent circuit fit values of solution resistance (R_{ele}), anode charge transfer resistance ($R_{anode,ct\ t}$) and anode double layer capacitance (C_{dl}) of LF-FC at various anode flow rates based on Figure 8 (A). (C) Impedance spectra for 0.05 M sulfuric acid added to the methanol solution. (D) The equivalent circuit fit values of solution resistance (R_{ele}), anode charge transfer resistance ($R_{anode,ct}$) and anode double layer capacitance (C_{dl}) of LF-FC at various anode flow rates based on Figure 8 (C).

acceptable 2% error for each circuit parameter. Figure 9C shows the anode electrochemical impedance spectra using the various flow rates of methanol in the presence of 0.05 M sulfuric acid. The Nyquist curves (impedance measurement) are essentially identical. Figure 9D shows the equivalent circuit results for 0.05 M sulfuric acid added to the methanol solution. It can be seen that the methanol flow rate does not influence its $R_{anode,ct}$ significantly. This tendency, seen in Figures 8 and 9, indicate that the addition of sulfuric acid in the anode fuel stream can eliminate the negative effect of high methanol flow rates.

Figures 9B and D also show that the C_{dl} is essentially unchanged at different methanol flow rates. This indicates that the width of the diffuse double layer (λ) is no longer affected by the bulk flow of the solution. According to equation (3), the addition of strong electrolytes, such as sulfuric acid, decreases the width of the diffuse double layer (λ) dramatically (in this case down to on the order of 1 nm) [27]. It should also be noted that due to the no slip condition, the bulk fluid velocity tends to zero at the electrode interface. We speculate that this extremely narrow width of the electrical double layer region is too close to the electrode surface to be substantially affected by the bulk flow. As a result, the anode performance and methanol oxidation kinetics of LF-FC are not significantly affected by the high methanol flow rate if sulfuric acid is present in the solution.

3.3. Effect of Concentration of H_2SO_4 on Methanol Oxidation Kinetics

Clearly the electrolyte strength of the fuel stream is important to the anode performance of LF-FCs. Figure 8 shows that at a 2 mL/min flow rate, the addition of sulfuric acid to the methanol

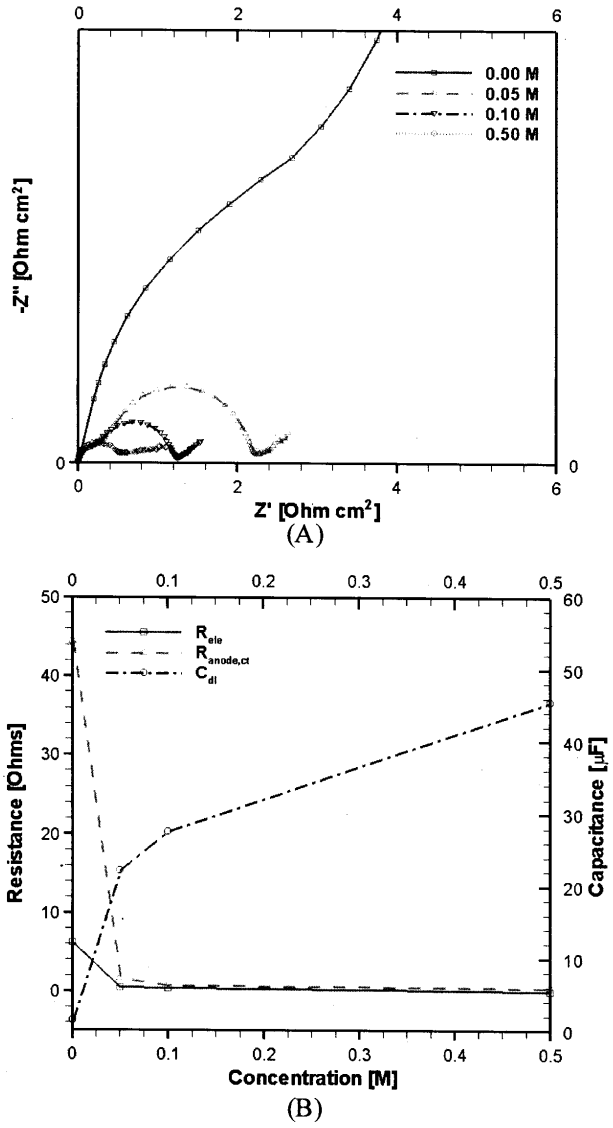

Figure 10. (A) Anode impedance spectra of LF-FC using the anode stream with the various concentrations of sulfuric acid. The methanol concentration was fixed at 1 M for the anode stream for all the measurements and the flow rate fixed at 2 μL/min. The PtBl cathode was supplied with 0.5 M sulfuric acid and served as the counter electrode. (B) The equivalent circuit fit values of solution resistance (R_{ele}), anode charge transfer resistance ($R_{anode,ct}$) and anode double layer capacitance (C_{dl}) of LF-FC at various anode flow rates based on Figure 10 (A).

solution decreases the onset potential of methanol oxidation by 200 mV from Figure 5. Also, the anode current output has increased over the entire applied anode potential range that we have studied. Figure 10 shows the effect of sulfuric acid concentration on the electrochemical impedance spectroscopy data. Figure 10.A shows the impedance spectra with different concentrations of sulfuric acid at 2 mL/min. It can be seen that a strong electrolyte greatly reduces the overall impedance of the anode. Figure 10.B shows the equivalent circuit fitting results. It should be noted that the use of the 0.5 M sulfuric acid fitted results is appropriate here. This is because the magnitude of the error is not large relative to the magnitude of the other sulfuric acid concentration data points. Therefore, the data could not be compared between the various flow rates but it can be compared to the other sulfuric acid concentration data sets as long as it is understood that there is some degree of inaccuracy in these values. The data shows that R_{ele} drastically decreases with increasing sulfuric acid concentration. Also, the value of C_{dl} increases as the electrolyte concentration increases from 0 to 0.5 M which is in accordance with well known double layer theory. The shape of the measured trend in C_{dl} is in excellent agreement with what the expected results from equations (2) and (3) would be. This assures that the electrochemical impedance spectroscopy is providing accurate results. Figure 10.B also shows that $R_{anode,ct}$ drastically decreases with increasing sulfuric acid concentration. Again, this is likely a result of the change in width of the diffuse double layer (λ) improving the driving force for methanol oxidation.

4. CONCLUSIONS

A micro scale laminar flow fuel cell was fabricated on PDMS and its anode performance was characterized using both the anode polarization and anode impedance analysis. In this study, 1 M methanol solutions, either with or without sulfuric acid as the supporting electrolyte, were supplied to the anode. In particular, the effects of methanol flow rate were investigated in both the presence and absence of a strong electrolyte, H_2SO_4, on its anode performance in terms of anode current density, onset potential of methanol oxidation, solution resistance (R_{ele}), anode charge transfer resistance, ($R_{anode,ct}$) and anode double layer capacitance (C_{dl}). In the absence of H_2SO_4, it was found that both the onset potential and $R_{andoe,ct}$ of methanol oxidation reaction increases as its flow rate increases. Changing values of the C_{dl} for different flow rate of the anode stream suggests that the anode double layer structure is affected by the anode flow rate. It can be argued that this change of the double layer structure and the resulting change in activation overpotential of electrokinetics over this double layer are the most likely causes of our observed decreasing methanol oxidation kinetics with an increasing flow rate of the anode stream in the absence of sulfuric acid. When 0.05 M – 0.5 M sulfuric acid is added to 1 M methanol anode stream, it was observed that the negative effects of high methanol flow rate on its oxidation kinetic is almost completely mitigated. The addition of sulfuric acid dramatically decreases the width of the anode diffuse double layer. A possible explanation is that the width is so thin in the presence of sulfuric acid that various flow rates of the anode stream do not significantly influence the width anymore, and hence that methanol oxidation kinetic does not decrease as the anode flow rate increases.

REFERENCES

[1] J. D. Morse, Int. J. Energy Res., 31, 576 (2007).
[2] R. Ferrigno, A. D. Stroock, T. D Clark, M. Mayer, G. M. Whitesides, J. Am. Chem. Soc., 124, 12930 (2002).
[3] E. R. Choban, P. Waszczuk, L. J. Markoski, A. Wieckowski, P. J. A. Kenis, J. of Power Sources, 128, 54 (2004).
[4] J. L. Cohen, D. A. Westly, A. Pechenik, H. D. Abruna, J. of Power Sources, 139, 96 (2005).
[5] S. Hasegawa, K. Shimotani, K. Kishi, H. Watanabe, Electro-

chemical and Solid-State Letters, 8, A119 (2005).
[6] J. L. Cohen, D. J. Volpe, D. A. Westly, A. Pechenik, H. D. Abruna , Langmuir, 21, 3544 (2005).
[7] E. R. Choban, J. S. Spendelow, L. Gancs, A. Wieckowski, P. J. A. Kenis, Electrochimica Acta, 50, 5390 (2005).
[8] E. Kjeang, A. G. Brolo, D. A. Harrington, N. Djilali, D. Sinton, J. of The Electrochemical Society, 154, B1220 (2007).
[9] E. Kjeang, B. T. Proctor, A. G. Brolo, D. A. Harrington, N. Djilali, D. Sinton, Electrochimica Acta, 52, 4942 (2007).
[10]R. S Jayashree, L. Gancs, E. R. Choban, A. Primak, D. Natarajan, L. J. Markoski, P. J. A. Kenis, J. Am. Chem. Soc., 127, 16758 (2005).
[11]R. S. Jayashree, D. Egas, J. S. Spendelow, D. Natarajan, L. J. Markoski, P. J. A. Kenis, Electrolyte Electrochemical and Solid-State Letters, 9, A252 (2006).
[12]M. H. Sun G. Velve Casquilas, S. S. Guo, J. Shi, H. Ji, Q. Ouyang, Y. Chen, Microelectronic Engineering, 84, 1182 (2007).
[13]E. Kjeang, J. McKechnie, D. Sinton, N. Djilali, J. of Power Sources, 168, 379 (2007).
[14]E. Kjeang, R. Michel, D. A. Harrington, N. Djilali, and D. Sinton, J. Am. Chem. Soc., 130, 4000 (2008).
[15]E. R. Choban, P. Waszczuk, P. J. A. Kenis, Electrochemical and Solid-State Letters 8, A348 (2005).
[16]K. G. Lim, G. Tayhas, R. Palmore, Biosensors and Bioelectronics, 22, 941 (2007).
[17]J. Zhang, Y. Tang, C. Song, J. of Power Sources, 163, 532 (2006).
[18]W. Jung, J. Han, S. Ha, J. of Power Sources, 173, 53 (2007).
[19]J. Qiao, M. Saito, K. Hayamizu, J. Electrochem. Soc., 153, A967 (2006).
[20]W. Chen, G. Sun, J. Guo, X. Zhao, S. Yan, J. Tian, S. Tang, Z. Zhou, Q. Xin, Electrochim. Acta, 51, 2391 (2006).
[21]K. Furukawa, K. Okajima, M. Sudoh, J. of Power Sources, 139, 9 (2005).
[22]T. Abe, H. Shima, K. Watanabe, Y. Ito, J. Electrochem. Soc., 151, A101 (2004).
[23]M. Chang, F. Chen, N. Fang, J. of Power Sources, 159, 810 (2006).
[24]R. F. Ismagilov, A. D. Stroock, P. J. A. Kenis, G. Whitesides, Appl. Phys. Lett., 76, 2376 (2000).
[25]E. Barsoukov, J. R. Macdonald, Impedance Spectroscopy Theory, Experiment, and Applications Second Edition, Wiley Inter-Science, New Jersey, 2005, pp 99.
[26]G. Prentice, Electrochemical Engineering Principles, Prentice-Hall, New Jersey, 1991.
[27]J. Newman, K. E. Thomas-Alyea, Electrochemical Systems Third Edition, Wiley Inter-Science , New Jersey, 2004, pp 276.
[28]J. Bockris, A. K. N. Reddy, Modern Electrochemistry; an Introduction to an Iinterdisciplinary Area, Plenum Press, New York, 1970.